IJST, Transactions of Electrical Engineering, Vol. 36, No. E1, pp 67-82
Printed in The Islamic Republic of Iran, 2012

DESIGN OF AN ADAPTIVE DYNAMIC LOAD SHEDDING ALGORITHM USING NEURAL NETWORK IN THE STEELMAKING COGENERATION FACILITY*

GH. ISAZADEH, R. HOOSHMAND** AND A. KHODABAKHSHIAN

Dept. of Electrical Engineering, University of Isfahan, Isfahan, I. R. of Iran
Email: hooshmand_r@eng.ui.ac.ir

Abstract– A new adaptive dynamic under frequency load shedding scheme for a large industrial power system with large cogeneration units is presented. The adaptive $LD\text{-}df/dt$ method with variable load shedding amount based on the disturbance magnitude is applied to have a minimum load shedding and a proper frequency recovery for different disturbances. To increase the speed of the load shedding scheme and to have an optimum response at different loading conditions, the artificial neural network (ANN) algorithm is developed. The Levenberg–Marquardt algorithm has been used for designed feed-forward neural network training. To prepare the training data set for the designed ANN, transient stability analysis has been performed to determine the minimum load shedding in the industrial power system at various operation scenarios. The ANN inputs are selected to be total in-house power generation, total load demand and initial frequency decay, while the minimum amount of load shedding at each step is selected for the output neurons. The proposed method is applied to the Mobarakeh steelmaking company (M.S.C) at different loading conditions. The performance of the presented ANN load shedding algorithm is demonstrated by the $LD\text{-}df/dt$ method. Numerical results show the effectiveness of the proposed method.

Keywords– Frequency stability, artificial neural networks, optimal load shedding, under-frequency relays

1. INTRODUCTION

For large industrial power systems, sudden separation from the utility grid is a major concern when the total plant load is much greater than the power output of the cogeneration units. To avoid a possible system collapse and to restore the system frequency it is necessary to apply load shedding in the industrial power system to maintain the system stability [1-2]. Conventional Load shedding schemes are designed for the worst anticipated scenario and are based on the utilization of discrete under-frequency relay (DUFR) [3]. The load shedding amount at different steps are constant with the predetermined time delays between different steps. Performance of these schemes is unreliable at severe disturbances with rapid frequency decay and system stability might be lost. Adaptive under frequency load shedding (AUFLS) plans are introduced based on disturbance magnitude [4-5]. The $LD\text{-}df/dt$ method based on the magnitude disturbance is introduced in [6] and compared with other possible adaptive load shedding methods. However, these approaches involve unacceptable time delays because of a need for time domain analysis at different loading conditions and disturbances. Because of the high dependency of the system frequency response on the initial operation condition, the seriousness of the fault contingency, the response of governor systems, and loads, it becomes more difficult to determine the minimum amount of the load shedding by the traditional methods in power systems. In this regard, it seems ANN can be an

*Received by the editors June 8, 2010; Accepted March 7, 2012.
**Corresponding author

ideal solution. Nowadays, the ANN algorithm is extensively used in power system analysis and design [7-9].

In this paper, a new adaptive under frequency load shedding scheme in a large industrial power system with cogeneration units is presented. First, the frequency settings of the protective relays for tripping the tie-lines are defined to isolate industrial power plant from utility network at external contingencies. By performing the transient stability analysis based on the $LD\text{-}df/dt$ method, the optimum amount of the load to be shed at different disturbances is determined. Total active power generation, total load and the value of df/dt at the time of isolation from the utility grid are considered as the input variables of the designed feed-forward neural network. The minimum amount of load shedding at each step according to the priority list of loads is selected as the output variables. Levenberg–Marquardt algorithm is used for training the ANN with training data set according to transient stability results. The proposed scheme has three advantages: 1) minimum amount of load to be shed, 2) adaptive load shedding according to the different loading conditions and disturbance magnitude and 3) fast and accurate response to different disturbances. The effectiveness of the proposed approach is demonstrated by time domain simulation on the M.S.C in the Isfahan Regional Electric Company (E.R.E.C) network with an in-house generation capability rating of 439MVA.

2. NEURAL NETWORK APPROACH

A multilayer feed-forward network with back propagation algorithm has been applied for the ANN training in this study. The two-layer feed-forward network is shown in Fig. 1 where the net input to unit h in the first layer is:

$$z(h) = \sum_{i=1}^{N_m} \omega_{ih} \cdot x_i + b_h \tag{1}$$

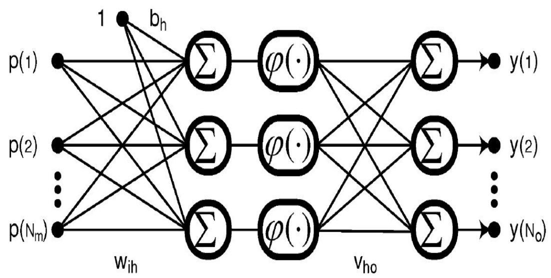

Fig. 1. Structure of a two-layered (or single-hidden-layer) feed-forward network

The net output from unit o in the second layer becomes:

$$y(o) = \sum_{h=1}^{N_h} \varphi(z(h)) \cdot v_{ho} \tag{2}$$

where ω_{ih} is the weight between input x_i and hidden unit, h, b_h is the bias term for the unit h which can be replaced by a weight with constant input, $\varphi(\bullet)$ is sigmoid function, v_{ho} is the weight between the hidden unit h and the output unit o, and N_h and N_m are the number of hidden units and the dimension of input space, respectively. In Levenberg–Marquardt algorithm (LMA), the performance index for the network is [10-11]

$$V = \frac{1}{2}\sum_{k=1}^{N_k} (\mathbf{t_k} - \mathbf{y_k})^T (\mathbf{t_k} - \mathbf{y_k}) = \frac{1}{2}\sum_{k=1}^{N_k} \mathbf{e_k}^T \cdot \mathbf{e_k} \tag{3}$$

where $\mathbf{t_k}$, $\mathbf{y_k}$ and $\mathbf{e_k}$ are the target, the output, and the error vector, respectively when the *k*th input vector $\boldsymbol{p}_k$ is presented. Let ω represent [$\boldsymbol{W;V}$] and then the batch weight estimation is defined as minimizing the argument of a criterion as follows:

$$[\hat{\boldsymbol{\omega}}] = \arg\min_{\boldsymbol{\omega}} \; V(\boldsymbol{\omega}) \tag{4}$$

Levenberg–Marquardt algorithm estimates the weights by approximating Newton's method. For the batch learning estimation given by (4), the Newton's method would be:

$$\Delta\omega = -[\nabla^2 V(\omega)]^{-1} \cdot \nabla V(\omega) \tag{5}$$

where $\nabla^2 V(\omega)$ and $\nabla V(\omega)$ are Hessian and gradient matrixes. If $V(\omega)$ is assumed to be a sum of square function, then it can be shown that:

$$\nabla V(\omega) = \mathbf{J}^{\mathbf{T}}(\boldsymbol{\omega}) \cdot \mathbf{e}(\boldsymbol{\omega}) \tag{6}$$

$$\nabla^2 V(\omega) = \mathbf{J}^{\mathbf{T}}(\boldsymbol{\omega}) \cdot \mathbf{J}(\boldsymbol{\omega}) + \mathbf{S}(\boldsymbol{\omega}) \tag{7}$$

where $\mathbf{S}(\boldsymbol{\omega}) = \sum_{k=1}^{N_k} \mathbf{e_k}(\boldsymbol{\omega}) \; \nabla^2 \mathbf{e_k}(\boldsymbol{\omega})$ and $\mathbf{J}(\boldsymbol{\omega})$ is the jacobian matrix. For the Gauss–Newton method, the Hessian matrix is approximated to $\mathbf{J}^{\mathrm{T}}\mathbf{J}$ by considering $\mathbf{S}(\boldsymbol{\omega}) \approx 0$. The Levenberg–Marquardt modification to Gauss–Newton is as follows:

$$\Delta\omega = [\mathbf{J}^{\mathbf{T}}(\boldsymbol{\omega}) \cdot \mathbf{J}(\boldsymbol{\omega}) + \mu \cdot \mathbf{I}]^{-1} \mathbf{J}^{\mathbf{T}}(\boldsymbol{\omega}) \cdot \mathbf{e}(\boldsymbol{\omega}) \tag{8}$$

where μ is the damping parameter and will be adjusted at each iteration. When μ is large, (8) becomes the gradient descent with a small step size. Newton's method is faster and more accurate near the minimum error and, therefore, the damping parameter is adjusted to shift toward Newton's method as quickly as possible. Thus μ is decreased after each successful step and is increased only when a step results in an increased $V(\omega)$. In this way, $V(\omega)$ would always be reduced at each iteration. The key step in the LMA is the computation of the Jacobian matrix. For the two-layered feed-forward network mapping problem, the Jacobian matrix can be computed by a simple modification of the back-propagation algorithm according to (9) [11].

$$\mathbf{J}(\bar{x}) = \begin{bmatrix} \frac{\partial e_1(\bar{x})}{\partial x_1} & \frac{\partial e_1(\bar{x})}{\partial x_2} & \cdots\cdots\cdots & \frac{\partial e_1(\bar{x})}{\partial x_m} \\ \frac{\partial e_2(\bar{x})}{\partial x_1} & \frac{\partial e_2(\bar{x})}{\partial x_2} & \cdots\cdots & \frac{\partial e_2(\bar{x})}{\partial x_m} \\ . & . & \cdots\cdots\cdots & . \\ \frac{\partial e_N(\bar{x})}{\partial x_1} & \frac{\partial e_N(\bar{x})}{\partial x_2} & \cdots\cdots & \frac{\partial e_N(\bar{x})}{\partial x_m} \end{bmatrix} \tag{9}$$

3. THE PROPOSED LOAD SHEDDING SCHEME

An optimal load shedding scheme must be adaptive to shed the minimum amount of load at different loading conditions according to magnitude of the disturbance. Initial slope of frequency decline (df/dt) is the only observable quantity that gives the size of disturbance magnitude [4-5]. The flowchart of the proposed optimal adaptive load shedding is shown in Fig. 2, and can be divided into five basic steps as follows:

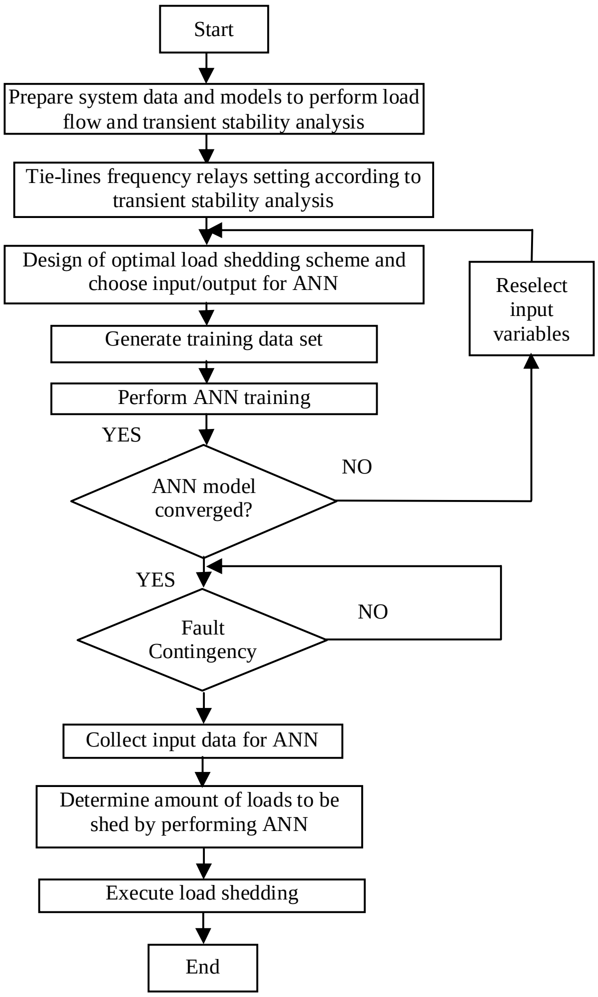

Fig. 2. Flowchart of ANN-based optimal load shedding

Step 1: System modeling; the system data is prepared for load flow and transient stability analysis including line and buses data and dynamic models for generators, exciter and governor systems, loads and reactive power compensators. Also, the priority list of loads in the system under study is defined.

Step 2: Tie-lines frequency protection setting; tie-lines frequency relays are set to isolate the industrial power system from the utility grid during external and internal disturbances, causing over or under frequency conditions. The over frequency setting is according to the critical clearing time of cogeneration units, while the under frequency setting is set properly to avoid cogeneration instability at under frequency situation in the utility grid.

Step 3: Optimal load shedding scheme is designed for many operation conditions in the system under study to obtain the minimum amount of the load to be shed at each loading condition. According to transient stability analysis, the load shedding frequency setting in the M.S.C system is determined. Then, the $LD\text{-}\,df/dt$ method is used to determine the minimum amount of the load to be shed at each step. The input variables are highly correlated to the frequency deviation as the training data of ANN models are chosen.

Step 4: ANN training; ANN training and testing are executed by using the feed-forward neural network structure with LMBP algorithm modified by Levenberg–Marquardt algorithm until the performance index is less than the specified error tolerance. The input variables are redefined if the ANN model does not converge.

Step 5: When a fault occurs, the proposed ANN method will determine the minimum amount of the load shedding quickly according to data gathered from the SCADA system in real time. The hardware will receive the amount of the load shedding predicted by the ANN controller to trip the predetermined load to restore the system frequency.

4. TRANSIENT STABILITY ANALYSIS

In this section, optimal load shedding scheme in the M.S.C power system (steps 2 and 3 of the flowchart) is designed for two different loading conditions according to Table 1. The case 1 is the severe loading condition, while M.S.C system is at peak load demand and the gas cogeneration unit is also out of service. In case 2, all cogeneration units are in service and the load demand is also at its peak value.

Table 1. Different loading condition of the M.S.C power system

Case	P_G(MW)	P_L(MW)	System operating condition
1	210	872	Peak load & 119 MW unit is out of service
2	329	872	Peak load & all units is in service

a) Power system description

The M.S.C is the largest integrated steelmaking company in the E.R.E.C network with four large cogeneration units. The M.S.C power system and its connection to the E.R.E.C network are shown in Fig. 3. It should be noted that although the whole transmission network of E.R.E.C is considered and simulated, this has not been shown in Fig. 3 for simplicity. The Chehelsoton power plant with a 1000 MVA capacity is very close to the M.S.C power system [12]. The M.S.C power system daily peak demand is about 872 MW while the maximum of total output power of cogeneration units is 329 MW, as shown in Table 2 [12]. According to the M.S.C operation record, the frequency of the isolated system will decline very quickly, and the cogeneration units will be tripped because of the failure of the generator auxiliary equipment. Therefore, it is very important to maintain the critical loads, such as generators, boilers, basic oxygen furnaces, etc., from suffering shutdown during the emergency state.

Table 2. Parameters of the M.S.C cogeneration units [12]

G1-G3 (Steam Uuits)				G4 (Gas unit)			
MVA	100	*MW*	70	*MVA*	135	*MW*	119
kV	15	*H*	2.6	*kV*	15	*H*	3.2
x_d	1.07	x'_d	0.187	x_d	1.53	x'_d	0.173
x''_d	0.11	T'_d	0.882	x''_d	0.117	T'_d	0.67
T''_d	0.035	x_q	1.04	T''_d	0.02	x_q	1.04
x'_q	0.375	x''_q	0.11	x'_q	0.364	x''_q	0.117
T'_q	0.64	T''_q	0.023	T'_q	0.64	T''_q	0.02

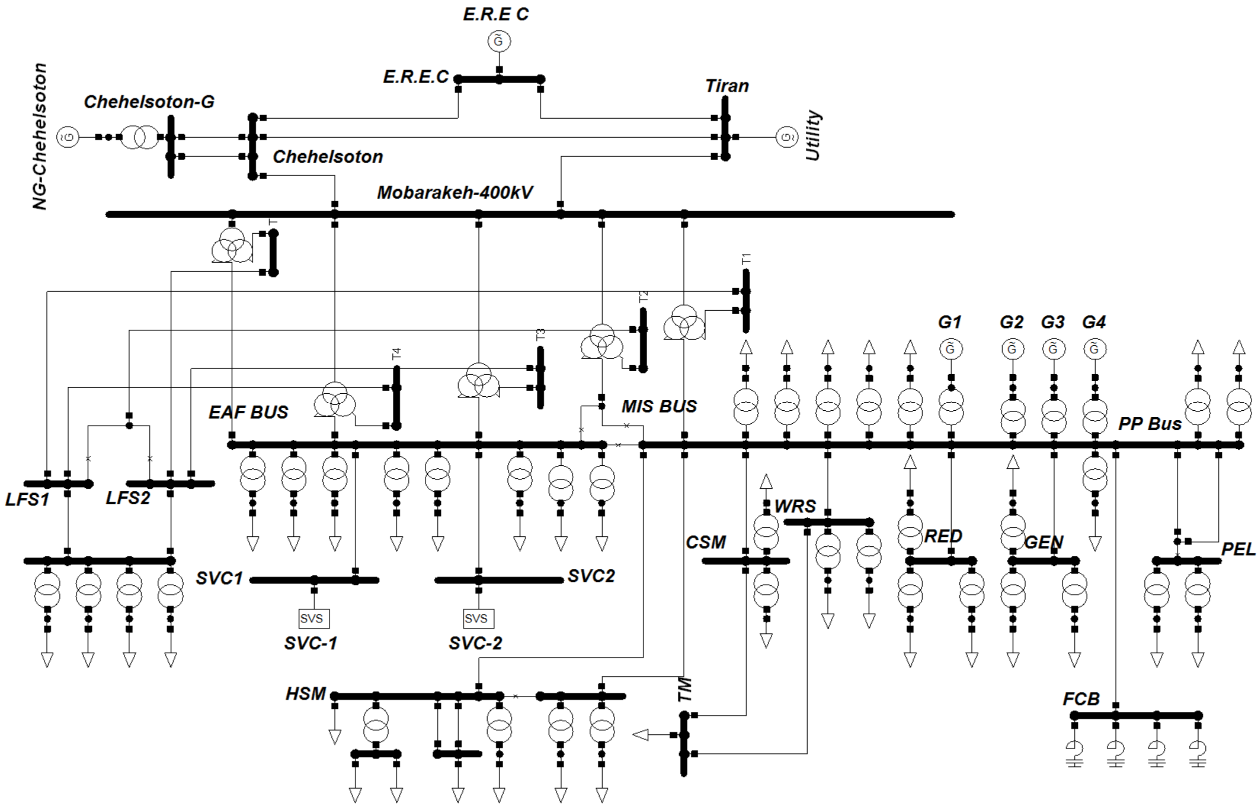

Fig. 3. M.S.C power system single line diagram

b) System modeling

To investigate the accurate transient behavior of the power system including generators, lines, loads, exciters, governor-turbine systems and reactive power compensators, the exact dynamic modeling of the apparatus must be derived. The apparatus that are modeled in the M.S.C system can be divided into five categories: 1) synchronous machines; 2) automatic voltage regulating (AVR) systems; 3) governor–turbine systems, 4) loads and 5) SVC which are considered as follows:

- Generator models: All M.S.C cogeneration units are represented by more detailed models, with transient and sub-transient circuits on both the direct and quadrate axes. The generators parameters are given in Table 2. The Chehelsoton and other generators in the E.R.E.C network are represented by only the transient circuits on both axes.

- Exciter models: The excitation systems of all cogeneration units corresponded to the IEEE type exciter models including type ST1A and type AC5A for steam and gas generators, respectively [13]. The saturation effect of excitation systems is included and expressed as an exponential function of field winding voltage (EFD). The parameters of exciters are shown in Appendix A.

- Governor models: The IEEE standard governor models are applied to the M.S.C and E.R.E.C generators [14]. Figures 4 and 5 show the governor systems for steam and gas turbines for both M.S.C and E.R.E.C generation units. The parameters of the governor systems are given in Appendix A.

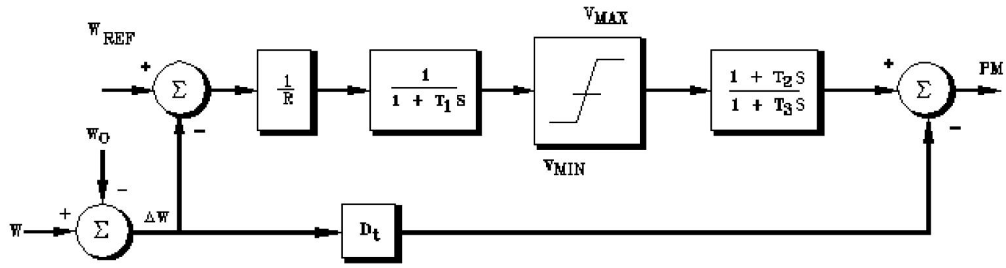

Fig. 4. Governor system for steam generator units in the M.S.C and E.R.E.C network

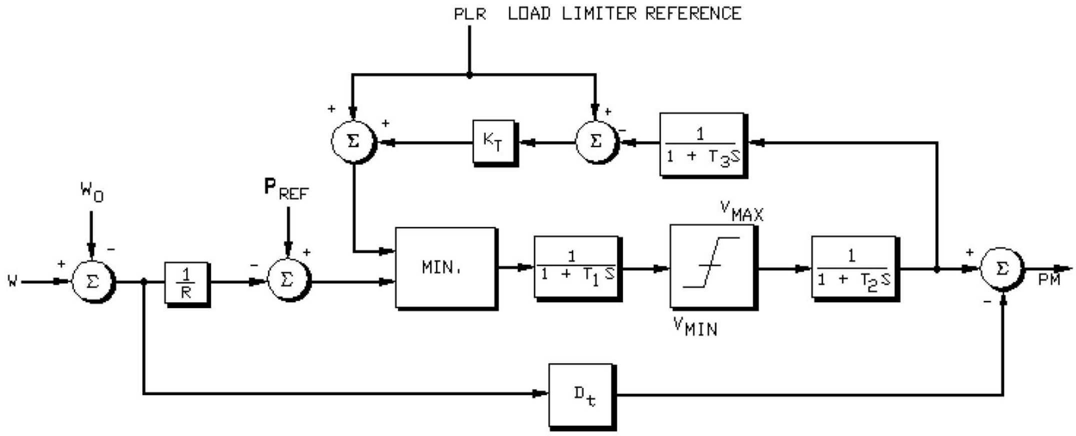

Fig. 5. Governor system for gas generator units in the M.S.C and E.R.E.C network

- Load models: Proper representation of load dynamic characteristics is a rather critical issue for transient stability analysis. The IEEE standard model is used for M.S.C power system loads modeling [15]. According to this model, the active and reactive part of the load can be represented by (10) and (11), both of which are voltage and frequency dependent.

$$P_L = P_0[a_1 V^{K1} + a_2 V^{K2} + a_3 V^{K3}]\ (1 + A_4 \Delta f) \tag{10}$$

$$Q_L = Q_0[a_5 V^{K1} + a_6 V^{K2} + a_7 V^{K3}]\ (1 + A_8 \Delta f) \tag{11}$$

According to the operation characteristics of various motor types, the decision has been made that the dc motors, which are controlled with electronic devices be treated as constant power load, while the operating voltages above the 480V and the 6.6kV ac motors are considered as constant impedance and constant current load, respectively. The parameters of the lighting loads and arc furnaces are based on the IEEE Std C37.117-2007 [15].

- SVC model: Two identical 100MVar SVCs are installed at the tertiary winding of two 400/63kV power transformers in the M.S.C system to achieve the following goals:

- Reactive power compensation and voltage stabilization.
- Fast response to the large variation of the reactive power demand of electrical arc furnaces (EAF).
- Flicker elimination to control the power quality parameters in the M.S.C and E.R.E.C power systems.

The SVC controllers in the M.S.C power system are shown in Fig. 6. It features a fast override control that applies either the maximum or minimum value of shunt reactor if the voltage error signal is larger than the threshold voltage (which is assigned as DV shown in Fig. 6). The controller parameters are given in Appendix A.

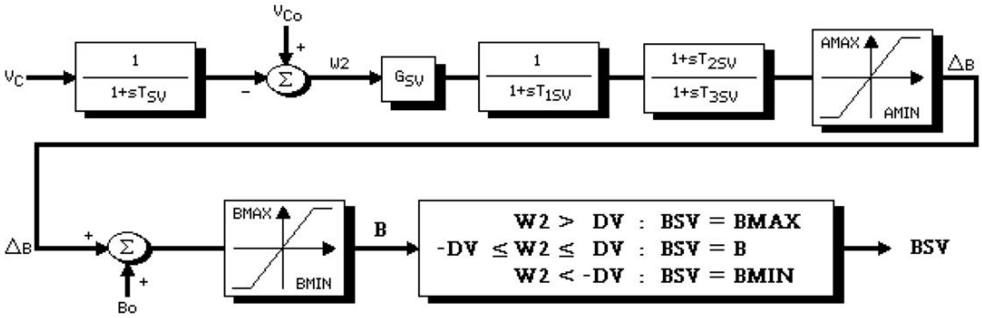

Fig. 6. SVC controller diagram in the M.S.C power system

c) Adaptive dynamic load shedding scheme

It is shown that the existing static load shedding with a constant load shedding amount and time delays between steps is unable to keep system stability at severe disturbances [16]. In this section an adaptive dynamic load shedding scheme based on the *LD-* df/dt method is designed [6]. However, in the proposed method, the total amount of load to be shed is determined with respect to the initial df/dt at the instant of M.S.C separation from the utility grid. Also, the load shedding amount is adaptive at each step. In other words, depending on the disturbance magnitude, a larger amount of loads is shed during the first steps for larger df/dt values. Therefore, the frequency setting for M.S.C tie lines tripping to isolate the industrial system for external disturbances is first discussed in section *A*. Then, the number of load-shedding steps and load shedding frequency settings in the M.S.C power system are determined in sections *B* and *C*. The load shedding amount based on the df/dt value is investigated in section *D* and the load shedding criteria is specified in Section *E*.

A. Determining the tripping frequency of tie-lines

In this section, the over and under frequency setting of M.S.C tie-lines based on the M.S.C cogeneration transient stability limit is determined. The nearby utility system fault will introduce a very low generator terminal voltage and this may result in instability in the M.S.C power system generators due to the mismatch of mechanical power and electric output power. Therefore, it is very important to identify the critical clearing time (CCT) of cogeneration units at external utility fault to determine the proper timing. In this situation, the Mobarakeh frequency reaches 51.2 Hz at 0.2 sec after fault occurrence according to tie-line tripping [17]. Based on transient stability analysis, the CCT for cogeneration units for a three-phase fault in the Mobarakeh-Chehelsoton 400kV line near to the 400kV Mobarakeh substation is 0.23s to stability studies. Thus, the over-frequency setting for tie-lines frequency relays are set to be 51.2 Hz to isolate the M.S.C system before cogeneration becomes unstable in an external fault condition. The under-frequency setting for the tie-lines tripping is selected to be 49.5Hz [2]. This setting is selected because the turbine-generator sets are not rated for continuous operation below 49.5Hz. Under-frequency tie-line tripping setting at this relative high value also tends to limit the maximum frequency deviation in severe loading conditions. According to transient stability analysis, df/dt value for the worst loading condition is -9 Hz/sec when the MSC power system is isolated from the grid. With respect to this high value, relays and circuit breakers time delays and the minimum allowable operating frequency of the generator turbine units, under-frequency setting for the tie-line tripping is selected to be 49.5Hz.

B. Choosing the number of load-shedding steps

It is known that a multi-step scheme is better than one step load shedding [1-2, 17]. In fact, tripping a big block of load at one time will have a large impact on a weak system. Therefore, a typical load shedding strategy with three shedding steps was adopted in this study.

C. Determining the tripping frequency for each shedding step

As mentioned earlier, load shedding is performed as soon as possible after separation of the M.S.C system from the E.R.E.C network. At first, with respect to the under-frequency setting for tie-line tripping (49.5Hz) and the df/dt value at the worst loading condition in the utility grid, the actual M.S.C system separation frequency is determined [4-6]. The first step of load shedding in the M.S.C system must be lower than this actual separation frequency. According to transient stability analysis, the highest anticipated df/dt value in the Iran utility grid is about 0.2 Hz/sec. Therefore, with 150msec time delay consideration for protection systems, the actual M.S.C separation frequency could be 49.2 Hz in the worst condition. So, the first step of under-frequency setting in the load shedding process in the M.S.C is selected to be 49.2Hz to coordinate frequency protection in the tie lines and M.S.C power system and perform the load shedding as soon as possible to keep the M.S.C system stability [18]. After the first step of load shedding is performed, the new value of df/dt is monitored and the setting of the second-step is determined with respect to the actual frequency of the first-step according to the new df/dt value and time delays. Similarly, the frequency setting of the third-step is determined. Therefore, frequency settings for the first-, second- and third-step of load shedding are selected to be 49.2, 48.6 and 48.2Hz, respectively with no time delay. The existing M.S.C load shedding frequency setting is 48.7, 48.2 and 47.6 Hz with constant load shedding at each step.

D. Amount of load to be shed

To avoid M.S.C power system collapse after isolation from the E.R.E.C network, it is necessary to curtail partial load to maintain the balance between available generation units and load as well as restoring the system frequency. To have a reliable scheme, the frequency decay rate as shown in (12) at the instant of tripping the tie-lines is used to derive the proper amount of load to be shed:

$$\Delta P = \frac{2H}{f_0} \cdot \frac{df}{dt} \tag{12}$$

where,

H_{sys} : Equivalent system inertia constant of the M.S.C system

f_0 : Nominal frequency of the system.

ΔP : M.S.C system overload in p.u.

Equivalent system inertia constant is calculated as follows:

$$H_{sys} = \frac{H_1.MVA_1 + H_2.MVA_2 + ... + H_n.MVA_n}{MVA_{sys}} \tag{13}$$

where *n* is the number of cogeneration units. Equivalent inertia constants in the M.S.C system for different cases as shown in Table 1 are 7.8 and 12.2 p.u on the system base of 100MVA. Inertia constants for cogeneration units in this study are given in Table. 2.

E. Criteria for acceptance load shedding performance

To have an effective and practical load shedding scheme, the following criteria is assigned in the designed scheme:

- After separation from the utility grid, the M.S.C frequency must be restored between 49.5–50.5Hz.
- Each generator steady-state MW and MVAR must not exceed its capability after load shedding has occurred.
- Generators must remain stable during and after the load shedding.
- The settings must ensure that all loads can be shed and removed before the generators are tripped.
- Steady state voltage at major buses, after the system recovers, must be between 95%–105% of nominal value.
- The minimum allowable frequency in the system is 47.5Hz.

5. ANN-BASED LOAD SHEDDING

Because of the dependency of the initial frequency decay rate (df/dt) to the power imbalance, total active power generation of cogeneration units (P_G), total load demand P_L and the initial frequency decay rate (df/dt) are considered as the input variables of the ANN model when tie-lines are disconnected. The output variables are defined as the minimum amount of load shedding, $P_{s\min}$ at each step based on the *LD-* df/dt method. The input/output pairs are, therefore, represented as:

$$\{\bar{p},\bar{q}\}=\left\{[P_G \;\; P_L \;\; \frac{df}{dt}]^T \;\;, [P_{S\min}]^T\right\} \tag{14}$$

The ANN construction in this study is shown in Table 3. The LMBP algorithm is applied to solve the ANN model with the performance index of 10^{-2} as the mean square error. The ANN is trained with the data training set which is obtained from transient stability analysis in 50 different scenarios at different M.S.C loading conditions. Among these 50 scenarios, 40 scenarios are used for training the ANN and the rest are utilized for testing cases. The performance index variation during 50 Epochs in the LMBP algorithm is shown in Fig. 7.

Table 3. The structure of the proposed ANN network

Input Neurons	3
Output Neurons	3
Hidden Layer	1
Neurons in Hidden Layer	10
NN Model	Feed-forward Network
NN Training Algorithm	Levenberg-Marquardt
Transfer Function	Tanh(x)
Max of Epochs	50
Performance Index	10^{-2}
Weight Up dates	Batch

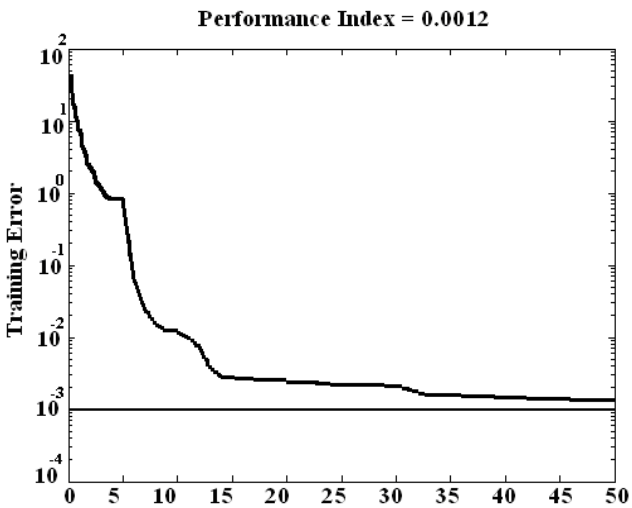

Fig. 7. Performance index variation in the LMBP algorithm

To evaluate the proposed method, the performance of two different algorithms (transient stability based on LD- df/dt and ANN method) is demonstrated at different conditions, including training and testing cases.

6. SIMULATION RESULTS

To increase the system reliability, the M.S.C power system is connected to two different substations in E.R.E.C network by two tie-lines. According to transient stability (T.S.) analysis, each of these tie-lines is adequate for supplying the M.S.C load demand when one of them becomes out of service due to fault or other contingencies. Therefore, load shedding scheme is activated when the M.S.C system is separated from the E.R.E.C network at special conditions. These special cases can be considered as under-frequency conditions due to external faults in the utility network, fault occurrence in the 400kV Mobarakeh substation or incorrect operation of the tie-lines protection relays. The LD-df/dt method is applied in transient stability analysis to have an optimal adaptive load shedding at different cases as given below. So, the transient stability results are based on the adaptive LD-df/dt method. The Digsilent Power Factory and MATLAB software have been used for M.S.C power system modeling and ANN training.

- Case 1

In this case study, M.S.C load demand is 872MW and steam cogeneration unit is out of service. Approximately 543MW active power is imported from the utility grid to the M.S.C system at this condition. It is assumed that a three-phase short circuit occurred at the 400kV Mobarakeh substation and M.S.C is isolated at 0.2 sec after this fault. The value of df/dt at the instant of isolation is -9 Hz/sec according to transient stability analysis. This high value is due to the peak load demand in the M.S.C system and a low equivalent inertia constant. The total amount of load to be shed is determined by (12) based on the initial df/dt value. After load shedding from the lower price of loads form priority list in Table 4, as step 1, the new value of df/dt is monitored. Other load shedding steps are calculated with respect to this new df/dt value and the priority list of loads. Table 5 shows the minimum amount of load to be shed in this case at different steps of load shedding scheme.

Table 4. Priority list of loads in the M.S.C power system

1	WRS, oxygen
2	Electrical arc furnace
3	Ladle furnace
4	PEL
5	RED
6	CSM, HSM

Table 5. Load shedding scheme in the M.S.C in case 1

$df/dt = -9$ Hz/sec		Priority of loads
Frequency setting	Amount of load to be shed (MW)	
49.2 Hz	294	CSM, HSM, RED
48.6 Hz	218	RED, PEL, EFS, LF, EAF
48 Hz	120	EAF

Figure 8 shows the frequency response of the M.S.C buses after load shedding. Load shedding scheme is activated and three steps of load shedding scheme are performed to limit the frequency decay and to restore it to the acceptable value. As can be seen from Table 5, three of the Electric Arc Furnaces (EAFs) loads must be shed from the priority list of load shedding. This is due to the severity of the disturbance and heavy loading condition in the M.S.C system for this case.

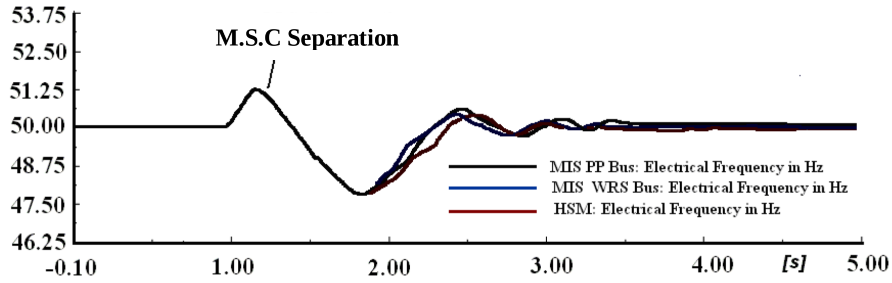

Fig. 8. Frequency response of M.S.C power system at case 1

- *Case 2*

In this case, like the previous one, M.S.C load demand is at peak value but all of the four cogeneration units are in service. Therefore, in this case, the initial df/dt value is lower than case 1. According to transient stability studies, df/dt value at the instant of M.S.C isolation is -3.1 Hz/sec. The minimum amount of load to be shed at different steps in this case is shown in Table 6. One of the EAF's and LF loads are shed in the third-step, while in case 1, three EAF's were disconnected in this step. Fig. 9 shows the frequency response of the M.S.C buses in this case.

Table 6. Load shedding scheme in the M.S.C in case 2

$df/dt = -3.1$ Hz/sec		Priority of loads
Frequency Setting	Amount of load to be shed (MW)	
49.2 Hz	234	CSM, HSM,
48.6 Hz	166	RED, PEL, EFS,
48 Hz	112	LF, EAF

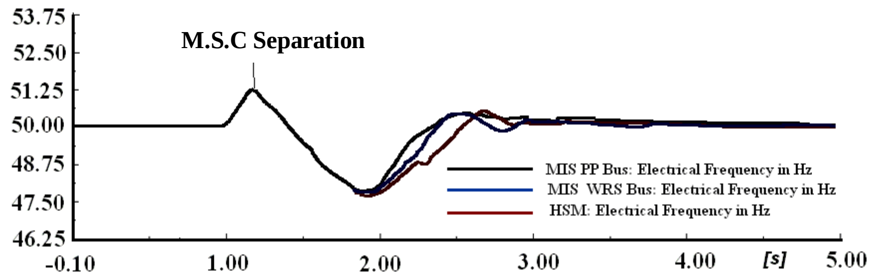

Fig. 9. Frequency response of M.S.C power system in case 2

- *Case 3*

In this case, the performance of the proposed ANN method is illustrated by the *LD-* df/dt method in case 1 which has been used for ANN training. Fig. 10 shows the frequency response of the M.S.C system at two different *LD-* df/dt and ANN based load shedding schemes in case 1. Table 7 demonstrates the amount of load to be shed at each step in two different analyses.

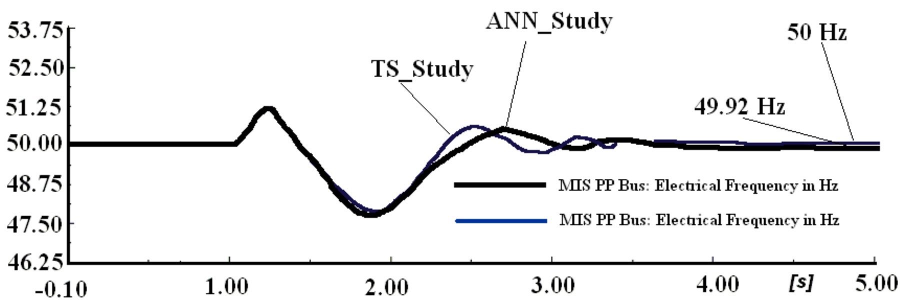

Fig. 10. Frequency response of M.S.C system in two different algorithms in case 3

Table 7. Amount of load to be shed in two different algorithms in case 3

$df/dt = -9$ Hz/sec		
Frequency Setting	Amount of load to be shed (MW)	
	Transient stability	ANN
49.2 Hz	294	264
48.6 Hz	218	232
48 Hz	120	118
Total Load shedding	632	614

- *Case 4*

In this case, the ANN performance is evaluated when one of 10 scenarios of testing cases is used. It is assumed that the load demand of the M.S.C power system from the utility is 490MW and the steam cogeneration unit is out of service. The df/dt value at the instant of isolation is -7.47Hz/sec at this condition. Fig. 11 shows the M.S.C power system frequency response from $LD\text{-}df/dt$ and ANN algorithm. Table 8 shows the minimum amount of load to be shed at each step of the two different methods.

- *Case 5*

Like the previous case, the performance of the ANN algorithm is demonstrated by $LD\text{-}df/dt$ method at different loading conditions from testing cases. Fig. 12 shows the frequency responses in two different algorithms. Table 9 shows the minimum amount of load to be shed obtained from two different algorithms. Numerical results obtained from transient stability and ANN algorithm at different loading conditions which were used for training are given in Table 10.

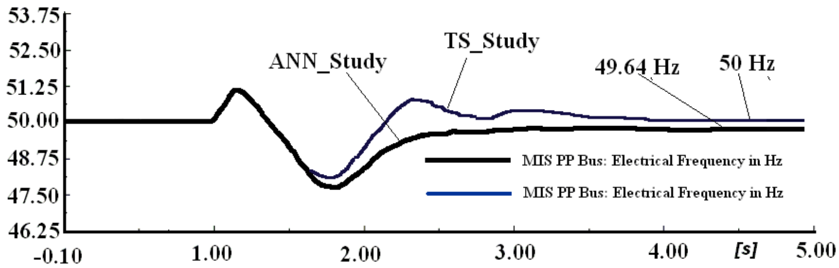

Fig. 11. Frequency response of M.S.C system in two different algorithms in different case 4

Table 8. Amount of load to be shed in two different algorithms in case 4

$df/dt = -7.47$ Hz/sec		
Frequency Setting	Amount of load to be shed (MW)	
	Transient stability	ANN
49.2 Hz	249	234
48.6 Hz	151	126
48 Hz	52	52
Total Load shedding	452	412

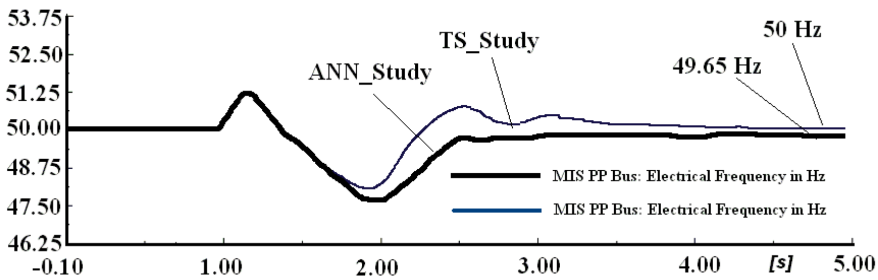

Fig. 12. Frequency response of M.S.C system in two different algorithms at different case5

Table 9. Amount of load to be shed in two different algorithms in case 5

$df/dt = -3.1\ Hz/\sec$		
Frequency Setting	Amount of load to be shed (MW)	
	Transient stability	ANN
49.2 Hz	234	234
48.6 Hz	165	126
48 Hz	52	40
Total Load shedding	452	400

Table 10. Numerical results in two different algorithms between ANN and transient stability (T.S) results

Frequency	Case 4			Case 5		
	T.S.	ANN	Abs. diff	T.S.	ANN	Abs. diff
Maximum positive deviation (Hz)	50.6	49.64	0.96	50.52	49.7	0.82
Maximum negative deviation (Hz)	48.34	47.59	0.75	48.3	47.58	0.72
Residual frequency(Hz)	50.00	49.64	0.36	50.00	49.65	0.35

- Amount of load shedding: With respect to the ANN results which are shown in Tables 7 to 9, the load shedding amount in the M.S.C power system for this algorithm is lower than the $LD\text{-}df/dt$ method. Consequently, because of the active power limitation of cogeneration units, the steady state frequency in the M.S.C buses is lower than 50Hz. However, as shown in Figs 10 to 12, the steady state frequency is above the pre-determined criteria for the minimum allowable frequency (49.5Hz) in the load shedding scheme. Also, the minimum transient frequency is higher than the 47.5 Hz in different cases.

- Computation burden

The total simulation time required for five seconds transient stability analysis in the M.S.C system including E.R.E.C network is about 45 seconds, while this time for the proposed ANN method for load shedding amount determination is much lower.

7. CONCLUSION

An adaptive optimal load shedding scheme by the ANN model with an LMBP algorithm was developed for the M.S.C system. By executing the transient stability analysis, the proper dynamic load shedding based on the adaptive LD-df/dt method with consideration to tie lines frequency protection setting is designed at different M.S.C operation scenarios. At severe disturbances with higher df/dt value, a higher number of loads have been shed at the first steps. The training data set of the ANN model, which consists of total system power generation, total load demand, frequency decay rate and the minimum amount of load shedding at each step, has been created. The performance of the proposed method has been demonstrated at different loading conditions in the M.S.C power system. It is concluded that the proposed ANN model with LMBP algorithm can solve the adaptive optimal load shedding at the instant of tie-line tripping by considering the real-time system operation scenario.

REFERENCES

1. Concordia, C., Fink, L. H. & Poullikkas, G. (1994). Load shedding on an isolated power system. IEEE Trans. Power Sys., Vol. 10, No. 3, pp. 1467-1472.
2. Anderson, P. M. & Mirheydar, M. (1992). An adaptive method for setting underfrequency load shedding relays. IEEE Trans. Power Sys., Vol. 7, No. 2, pp. 647-653.
3. Hsu, C. T., Chen, C. S. & Chen, J. K. (1997). The load shedding scheme design for an integrated steel making cogeneration facility. *IEEE Trans. Ind. Appl.*, Vol. 33, No. 3, pp. 586-592.

4. Terzija, V. V. (2006). Adaptive underfrequency load shedding based on the magnitude of the disturbance estimation. *IEEE Trans. Power Sys.*, Vol. 21, No. 3, pp. 1260-1266.
5. Terzija, V. V. & Koglin, H. J. (2002). Adaptive underfrequency load shedding integrated with a frequency estimation numerical algorithm. *IEE Proc.-Gener. Transm. Distrib*, Vol. 149, No. 6, pp. 713-718.
6. Seyedi, H., Sanaye-Pasand, M. (2009). Design of new load shedding special protection schemes for a double area power system. American Journal of Applied Sciences, Vol. 6, No. 2, pp. 317-327.
7. Seifi, H. & Pedram, M. M. (1999). A self-tuned fuzzy set based power system stabilizer with the aid of genetic algorithms and artificial neural networks. *Iranian Journal of Science and Technology, Transaction B: Engineering*, Vol. 23, No. 1, pp. 1-10.
8. Mohan Saini, L. & Kumar Soni, M. (2002). Artificial neural network-based peak load forecasting using conjugate gradient methods. *IEEE Trans. Power Sys.*, Vol. 17, No. 3, pp. 907-912.
9. Swiatek, B., Rogoz, M. & Hanzelka, Z. (2007). Power system harmonic estimation using neural networks. 9th *International Conference on Electrical Power Quality and Utilization*, pp. 1-8.
10. Hsu, C.T., Kang, M. S. & Chen, C. S. (2005). Design of adaptive load shedding by artificial neural networks. *IEE Proc.-Gener. Transm. Distrib*, Vol. 152, No. 3, pp. 415–421.
11. Hagan, M. T. & Menhaj, M. B. (1994). Training feed-forward networks with the marquardt algorithm. *IEEE Trans. Neural Net.*, Vol. 4, No. 5, pp. 989-993.
12. IGMC Report, System planning Study in the IRAN Power Grid at the year of 2015.
13. IEEE Std 421.5-2005: (2006). IEEE recommended practice for excitation system models for power system stability studies.
14. IEEE Committee Report. (1973). Dynamic models for steam and hydro turbines in power system studies. *IEEE Trans. Power Apparatus and Sy*s., Vol. 92, No. 6), pp. 1904–1915.
15. IEEE Std. C37.117: (2007). IEEE guide for the application of protective relays used for abnormal frequency load shedding and restoration. pp. 1-43.
16. Final report of M.S.C power system Blackout in the years of 2003 and 2006, (2008), MSC Research group.
17. Chen, C. S., Hsu, C.T. & Ke, Y. L. (2000). Protective relay setting of the tie-line tripping and load shedding for the industrial power system. *IEEE Trans. Ind. Appl.*, Vol. 36, No. 5, pp. 1226-1234.
18. ANSI/IEEE Std. C37.010: (1979). Application guide for AC high-voltage circuit breakers rated on a symmetrical basis.

APPENDIX A: PARAMETERS OF THE M.S.C POWER SYSTEM

a) Exciter system parameters of generators

a-1) G1-G3 Exciter parameters

T_R= 0.012 sec ; T_C= 1 sec ; T_B= 1 sec ; T_{C1}= 0 sec ; T_{B1}= 0 sec ; K_A= 200 ; T_A= 0.02 sec
V_{IMAX}= 2.9 ; V_{IMIN}= -2.9; V_{AMAX}= 3.15 ; V_{AMIN}= -2.52 , K_C= 0 ; K_F= 0.2 ; T_F= 1 sec
K_{LR}= 0 ; I_{LR}= 0 , V_{RMAX}= 3.15 ; V_{RMIN}= -2.52

a-2) G4 Exciter parameters

T_R= 0.012 sec ; T_A= 0.02 sec ; K_F= 0.045 ; T_F= 0.69 sec ; K_A= 400 ; K_E= 1 ; T_E= 0.75 sec
$SE\ (E1)$= 0 ; $SE\ (E2)$= 0.1 ; $E2$= 4.576 , VR_{Max}= 4.576 ; VR_{Min}= -3.66 ; T_B= 0.0 sec ; T_C= 0.0 sec

b) Governor system parameters of generators

b-1) G1-G3 Governor parameters

R= 0.05 p.u. ; T_1= 0.5 sec ; T_2= 1.25 sec ; T_3= 1.4 sec ; V_{MAX}= 0.8 p.u. ; V_{MIN}= 0.0 p.u. ; D_{turb}= 0.0

b-2) G4 Governor parameters

R= 0.05 p.u. ; T_1= 30.0 sec ; T_2= 1.0 sec ; T_3= 3.0sec ; K_T= 2.0 ;
V_{MAX}= 0.815p.u. ; V_{MIN}= 0.0p.u. ; D_{turb}=0.0

c) SVC controller parameters

T_{SV}= 0.0167 sec ; T_{1SV} = 0.13 sec ; G_{SV} = 91 ; T_{2SV}= 0.0 sec ; T_{3SV}= 0.0 sec
A_{MAX}= 3.64 , A_{MIN} = -3.64 ; B_{MAX}= 2.66 ; B_{MIN} = -0.98 ; D_V= 0.1

d) Active and reactive parts of M.S.C loads

Table A-1. Active and reactive parts of M.S.C loads

Bus	MW	MVAR
LFS		
LF1/4	52	37
EAF		
EAF1+EAF2+EAF7+EAF8		
EAF5+EAF6	240	168
EAF3 and EAF4 (Spare)	120	90
MIS		
T1BM	15	12
T2BM	15	12
CSM		
T1BC	15	13
T2BC	15	13
T3BC	14.5	13
T4BC	14.5	13
Existing Tandem	25	25
New Tandem	17	17
EFS		
T1BE	20	12
T2BE	20	12
HSM		
T1BH	16	14
T2BH	16	14
T3BH	16	16.5
R1+NEW R3	20	10
F1/6+F7	65	45
RED		
T1BR	15	11.5
T2BR	15	11.5
T3BR	15	11.5
T4BR	15	11.5
T5BR	15	11.5
T6BR	16	12
PEL		
T1BP	17.5	12.5
T2BP	17.5	12.5
GEN		
T12BG	12	9
T32BG	12	9
WRS		
T1BW	3	3
T2BW	3	3